Autographa californica multiple nucleopolyhedrovirus *orf114* is not essential for virus replication in vitro, but its knockout reduces *per os* infectivity in vivo

Wenqiang Wei · Yin Zhou · Chengfeng Lei · Xiulian Sun

Abstract *Autographa californica* multiple nucleopolyhedrovirus (AcMNPV) *orf114* (*ac114*) is one of the highly conserved unique genes in the lepidopteran group I nucleopolyhedrovirus. So far, the biological function of *ac114* is unknown. To study the function of *ac114* in the virus life cycle, an *ac114* knockout baculovirus shuttle vector (bacmid) was generated. Fluorescence and light microscopy showed that the *ac114* knockout mutant was able to produce infectious budded viruses (BVs) and occlusion bodies (OBs). Titration assays demonstrated that the *ac114* knockout virus had similar growth kinetics to the control virus during the infection phase. Electron microscopy indicated that *ac114* did not affect the morphogenesis of BVs and occlusion-derived viruses (ODVs); however, the numbers of ODVs per OB of the *ac114* knockout virus were significantly lower than those of the control virus. RT-PCR demonstrated that *ac114* was a late stage expression gene and that its transcription initiated at an A residue, 16 nucleotides upstream of the ATG start codon. Intracellular localization analysis revealed that the Ac114-GFP fusion protein localized predominantly as punctate patches in the cytoplasm of infected Sf9 cells. Bioassays showed that the *ac114* knockout did not change the killing speed of AcMNPV in *Spodoptera exigua* larvae, but reduced its viral infectivity significantly. Taken together, these data indicate that *ac114* is an auxiliary gene that facilitates embedding of ODVs into OBs, thus affecting the *per os* infectivity of the virus.

Keywords *Autographa californica* multiple nucleopolyhedrovirus · *ac114* knockout · Replication · Infectivity

W. Wei · Y. Zhou · C. Lei · X. Sun (✉)
Key Laboratory of Agricultural and Environmental
Microbiology, Wuhan Institute of Virology, Chinese Academy
of Sciences, Wuhan 430071, China
e-mail: sunxl@wh.iov.cn

W. Wei
e-mail: greatdream168@yahoo.com.cn

Y. Zhou
e-mail: zhouyin@wh.iov.cn

C. Lei
e-mail: cflei@wh.iov.cn

W. Wei
Graduate University of Chinese Academy of Sciences,
Beijing 100039, China

Introduction

Members of the *Baculoviridae* family can infect larvae within the orders Lepidoptera, Hymenoptera, and Diptera; the family consists of four genera, namely, the alpha-, beta-, gamma-, and delta-baculoviruses [1]. Alphabaculoviruses are Lepidoptera-specific nucleopolyhedroviruses (NPVs) that can be divided into two groups known as group I and group II as based on phylogenetic studies [2, 3]. The *Autographa californica* multiple nucleopolyhedrovirus (AcMNPV) genome is approximately 134 kbp and contains 154 predicted open reading frames (orfs) [4]. Comparative analysis of the 40 or so baculovirus genomes completely sequenced to date has revealed 30 conserved core genes. These genes are central to DNA replication, RNA transcription, nucleocapsid assembly, and budding off of the virus [5]. There are some unique genes that only exist in the group I NPV, including *gp64*, *ie2*, *ptp1*, *odv-e26*, *ac5*, *ac30*, *ac72*, *ac73*, *ac114*, *ac124*, and *ac132* [5]. These genes have been found to be involved in various processes such as cellular attachment (*gp64*) [6], viral DNA

replication and gene expression (*ie2*) [7], larvae locomotion (*ptp1*) [8], and transcription regulation (*ac16*) [9]. However, thus far, several unique genes (i.e., *ac72*, *ac114*, *ac124,* and *ac132*) remain uncharacterized.

AcMNPV *orf114* (*ac114*) is predicted to encode a protein of 424 amino acids with a molecular mass of 49 kDa. Mass spectrometry has shown that the Ac114 protein is associated with AcMNPV BV and occlusion-derived virus (ODV) particles [10, 11]. Evolutionary rate analysis has shown that within the *ac114* gene the average ω and K_a values were around two times lower than that of the *gp64* gene, suggesting that *ac114* has evolved under relatively relaxed purifying selection [12]. Phylogenetic analysis has also revealed that Ac114 shares homology with a hypothetical protein from the human malaria parasite *Plasmodium falciparum* (3D7 strain) [13]. HHpred analysis predicted that Ac114 contains the general transcription factor II-I repeat domain that is involved in signal-dependent transcription regulation in various biological contexts [14]. However, information on the function of *ac114* or any of the other homologs in the baculovirus life cycle is currently limited.

In this study, an *ac114* knockout bacmid was generated using an AcMNPV bacmid. The effects of the *ac114* knockout on the production of budded viruses (BVs) and occlusion bodies (OBs), temporal transcription, cellular localization, and the infectivity of OBs were examined.

Materials and methods

Virus, cell lines, and insects

The AcMNPV bacmid bMON14272 (Invitrogen Life Technologies, Carlsbad, CA, USA) was derived from AcMNPV, which could propagate in *Escherichia coli* DH10B cells. Sf9 cells were cultured at 27 °C in Grace's medium (Invitrogen) supplemented with 10 % fetal bovine serum (Gibco, Grand Island, NY, USA). *Spodoptera exigua* larvae were reared on an artificial diet [15] at 28 °C.

Construction of *AcMNPV* bacmids containing enhanced green fluorescence protein (gfp) and polyhedrin

The *ac114* knockout bacmid was constructed using the λ-recombination system in *E. coli* as previously described [16]. First, the chloramphenicol resistance gene (Cm) was amplified from the pKD3 plasmid by PCR with primers ac114-KO-F and ac114-KO-R (Table 1), which contained a 40 bp fragment homologous to one terminus of hr4B and the 3′ terminus of *ac115*, respectively, in accordance with the 97,886–97,925 and 99,121–99,160 nt positions within the AcMNPV genome (NC 001623.1) [4], to preserve the functions of hr4b and *ac115*. The gel-purified Cm cassette PCR fragment was electroporated into *E. coli* BW25113 harboring the AcMNPV bacmid bMON14272 and pKD46

Table 1 List of primers

| Primer name	Primer sequence
ac114-KO-F	TTACAGCACTTCGTAGTTGTATCGAAAATTGTT CAATGGCTGTAGGCTGGAGCTGCTT
ac114-KO-R	ATGAGCAAGTACGCGCTTTTACAAAAAATGATC ATCAACGCATATGAATATCCTCCTT
ac114-F	TGTTCATTGAACCGGTTAC
ac114-R	CGGCGCTATAAATGCATC
ac114-IN-F	TGAGCACGCTACTGGAAG
ac114-IN-R	GTAATCCCGTTCATACGC
Cm-F	CATATGAATATCCTCCTTAG
Cm-R	TGTAGGCTGGAGCTGCTTCG
ac114-Orf-F	CCGGAATTCATGAGCAAGTACGCGCTT
ac114-Orf-R	GCTCTAGACAGCACTTCGTAGTTGTATCG
aclef3-F	ATGGCGACCAAAAGATCT
aclef3-R	CAAAAATTTATATTCATTTTCATC
GSP1	GGTGATTGAGCGAGGTTTGAG
GSP2	CATTGCCGTCTTCCAGTAGC
M13-F	CCCAGTCACGACGTTGTAAAACG
M13-R	AGCGGATAACAATTTCACACAGG
gfp-F	GTCTCTAGAATGGTGAGCAAGGGCGAGGAGC
gfp-R	GACAAGCTTCTTGTACAGCTCGTCCATGCCGAG
polyhedrin-F	CTAGCTAGCACCATCTCGCAAATAAATAAG
polyhedrin-R	TATGCATGCTGTATCGTGTTTTAATACGCC

(encoding the λ-Red recombinase). After incubation at 30 °C in 0.8 ml of SOC medium [17] for 2 h, the electroporated cells were spread onto agar plates with medium containing 50 μg/ml of kanamycin and 25 μg/ml of chloramphenicol. The plates were incubated at 37 °C for 2–3 days and colonies were selected for PCR analysis. The replacement of *ac114* by the Cm cassette was confirmed using the primers ac114-F/ac114-R and Cm-F/Cm-R (Table 1). The recombination junctions between the Cm cassette and the flanking sequences of *ac114* were examined using the ac114-F/Cm-R and Cm-F/ac114-R primers (Table 1). A 1,195 bp fragment of the *ac114* coding region in the AcMNPV bacmid was replaced with the Cm cassette to produce AcMNPV$^{ac114\text{KO}}$ph$^-$ (Fig. 1a).

The AcMNPV bacmid bMON14272 has an occlusion-minus phenotype [17]. To obtain bacmids containing the

polyhedrin and *gfp* genes, the donor plasmid Dual-gfp-ph was constructed. In brief, the *gfp* PCR product, amplified from pEGFP-N1 (Clontech, Heidelberg, Germany) with the primers gfp-F and gfp-R (Table 1), was digested with *Xba*I and *Hin*dIII and ligated into pFastBacDual (Invitrogen), downstream of the *polyhedrin* promoter, to generate Dual-gfp. Subsequently, the *polyhedrin* PCR product, amplified from AcMNPV (C6) genomic DNA with the primers polyhedrin-F and polyhedrin-R (Table 1), was digested with *Sph*I and *Not*I, and cloned into Dual-gfp under the control of a *p10* promoter, to generate Dual-gfp-ph. Thereafter, the donor plasmid Dual-gfp-ph was transformed into electrocompetent DH10B cells containing the helper plasmid pMON7124 and bacmid AcMNPV$^{ac114\text{KO}}$ph$^-$ (or bMON14272) to generate the bacmid AcBac-*ac114*KO (or AcBac) (Fig. 1c). After incubation at 37 °C for 4 h in 0.8 ml of SOC medium,

Fig. 1 Generation of the *ac114* knockout and wild-type AcMNPV bacmids. **a** Construction strategy for AcMNPV$^{ac114\text{KO}}$ph$^-$. The partial coding region of *ac114* in AcMNPV bMON14272 was replaced with the chloramphenicol resistance gene (Cm) by homologous recombination in *E. coli*. **b** PCR confirmation of *ac114* knockout bacmid. The primer pairs are indicated above each line. Sizes markers are indicated on the *right*-hand side of the panel. **c** Schematic diagram of the recombinant bacmids AcBac and AcBac-*ac114*KO, showing the *polyhedrin* (*polh*) and *enhanced green fluorescent protein* (*gfp*) genes inserted into the *polyhedrin* locus of AcMNPV bMON14272 or AcMNPV$^{ac114\text{KO}}$ph$^-$ by Tn7-mediated transposition. **d** Verification of the *ac114* knockout by RT-PCR. Total RNA was extracted from mock-infected Sf9 cells (Mock), or Sf9 cells infected with either vAcBac (wt) or vAcBac-*ac114*KO (KO). RT-PCR was conducted using the primers ac114-Orf-F and ac114-Orf-R flanking the *ac114* knockout region, and ac114-IN-F and ac114-IN-R within the knockout region. DNA size markers are shown on the *right*-hand side
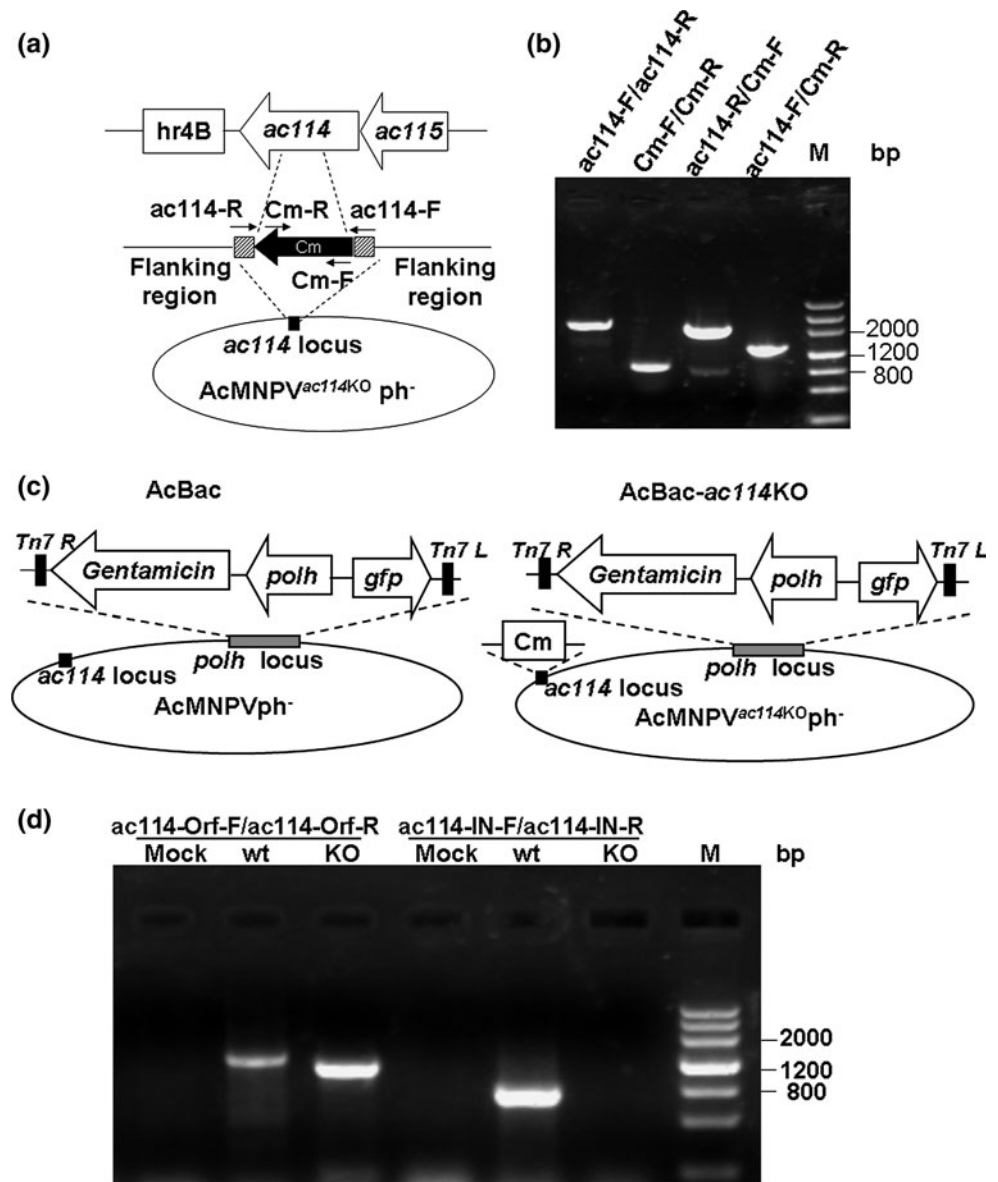
DH10B cells were plated onto LB agar medium containing 50 μg/ml of kanamycin, 7 μg/ml of gentamicin, 10 μg/ml of tetracycline, 100 μg/ml of X-Gal, and 40 μg/ml of IPTG. The plates were incubated at 37 °C for 48 h, white colonies were selected, and the presence of the correct construct confirmed by PCR using universal M13-F/M13-R primers (Table 1).

Transfection of cells and virus growth curves

Sf9 cells (1.0×10^6 cells/35-mm-diameter plate) were transfected with 2.0 μg of the recombinant bacmids AcBac or AcBac-ac114KO using 8 μl of Cellfectin reagent (Invitrogen) according to the manufacturer's instructions. After incubation for 4 h, the transfection supernatants were discarded and the cells were replenished with 2 ml of fresh Grace's medium (Invitrogen) supplemented with 10 % fetal bovine serum, 100 μg/ml of penicillin, and 30 μg/ml of streptomycin. Green fluorescent protein (GFP) expression and OB formation were observed by fluorescence microscopy. Supernatants containing BVs (designated vAcBac or vAcBac-ac114KO) were collected at 72 h post-transfection (p.t.) and the BV titers were determined by end-point dilution assays in Sf9 cells.

To determine the kinetics of BV production, Sf9 cells (1.0×10^6 cells/35-mm-diameter plate) were infected with vAcBac or vAcBac-ac114KO at a multiplicity of infection (MOI) of 5. At designated time points (i.e., 0, 12, 24, 48, 72, and 96 h post-infection (p.i.)), the supernatants were harvested from the infected cells and centrifuged at $8,000 \times g$ for 5 min to remove the cell debris. The BV titers were determined by end-point dilution assays on Sf9 cells in triplicate using 96-well microtiter plates. The BV titers of the recombinant viruses at each time point were compared using a Student's *t* test after logarithm transformation.

Transmission electron microscopy

Sf9 cells (1.0×10^6 cells/35-mm-diameter plate) were infected with each BV (vAcBac, vAcBac-ac114KO) at a MOI of 5. At 96 h p.i., the supernatants were discarded, the cells were then pelleted, fixed in 2.5 % glutaraldehyde at 4 °C overnight, washed three times with 0.1 M PBS (pH 7.2), followed by fixation in 1 % osmium tetroxide for 2–3 h at room temperature. After dehydration in graded ethanol (30–100 %), cells were soaked in acetone and embedded in spur resin. After staining with uranyl acetate and lead citrate, ultrathin sections were examined using a Hitachi H-800 transmission electron microscope (Hitachi Co., Ltd., Tokyo, Japan).

To determine whether a lack of *ac114* had any effect on the number of ODVs embedded in one OB, OBs isolated from vAcBac- or vAcBac-ac114KO-infected *S. exigua* larvae were alkali-treated and the ODVs with an intact envelop were counted using electron microscopy as previously described [18]. ODV counts per OB of the two viruses were transformed into square roots to normalize the data and compared by a Student's *t* test.

Total RNA extraction and reverse transcription (RT)-PCR

Sf9 cells (1.0×10^6 cells/35-mm-diameter plate) were infected with AcMNPV at a MOI of 5. Total intracellular RNAs were isolated from mock- and viruses-infected cells at 0, 6, 9, 18, 24, 48, and 72 h p.i. using TRIZOL (Invitrogen). The extracted RNA samples were treated with RNase-free DNase I (TaKaRa Biotechnology Co., Ltd., Dalian, China) to remove genomic DNA contamination. The First-strand cDNA was synthesized using reverse transcriptase (Invitrogen) and an oligo(dT) primer (TaKaRa) with 2 μg total RNA as template. The cDNA mixtures were amplified using the *ac114* primers ac114-Orf-F/ac114-Orf-R (Table 1). Another reaction that included no RT prior to PCR amplification was used as a control to detect any possible viral DNA contamination. The AcMNPV *lef3* gene was amplified with the primers aclef3-F/aclef3-R (Table 1) and used as a control. PCR products were analyzed on 0.8 % agarose gels.

The 5′ ends of the *ac114* transcripts were determined using total RNA harvested at 24 h p.i. According to the manufacturer's protocol from the 5′ full RACE kit (TaKaRa), the first-strand cDNA was synthesized with the random primer (TaKaRa). After the cDNAs were generated, the RACE-PCRs were conducted with the *ac114*-specific primer GSP1/5′ RACE outer primer (TaKaRa) followed by the GSP2/5′ RACE inner primer (TaKaRa). The PCR products were gel purified and cloned into pMD-18T (TaKaRa) for sequencing.

To verify the knockout of *ac114* from AcMNPV, RNAs were isolated from vAcBac- or vAcBac-ac114KO-infected Sf9 cells as described above. RT-PCR was carried out using primers ac114-Orf-F/ac114-Orf-R flanking the *ac114* knockout region and ac114-IN-F/ac114-IN-R (Table 1) spanning the *ac114* knockout region.

Subcellular localization of Ac114 during viral infection

To monitor the localization of Ac114 in Sf9 cells, a recombinant bacmid containing the Ac114-GFP chimera was constructed. The *ac114* orf (without the TAA stop codon) was amplified from the AcMNPV bacmid with primers ac114-Orf-F and ac114-Orf-R (Table 1). The *ac114* PCR product was digested with *Eco*RI and *Xba*I and

cloned into Dual-gfp-ph in frame with the *gfp* gene to generate Dual-*ac114*-gfp. Dual-*ac114*-gfp was transformed into DH10B cells, which contain the helper plasmid pMON7124 and bacmid AcMNPV$^{ac114\text{KO}}$ph$^-$ to generate AcBac-*ac114*Rep (Fig. 7a). Sf9 cells were transfected with the bacmid AcBac-*ac114*Rep, and the BVs (designated vAcBac-*ac114*Rep) harvested from the supernatant of the transfected cells were used to infect Sf9 cells at a MOI of 5. The vAcBac-*ac114*KO construct was used as a control. At 96 h p.i., cells were stained with Hoechst 33258 and visualized with fluorescence microscopy (Zeiss, Oberkochen, Germany).

Bioassays

The median lethal dose (LD$_{50}$) of the AcMNPV variants and median survival time (ST$_{50}$) of the third-instar *S. exigua* larvae inoculated with the viruses were determined by a droplet-feeding assay as described previously [18]. The LD$_{50}$ assay was conducted by incubating the groups of 48 larvae with different doses of the OB suspensions for 10 min. The larvae that ingested the OBs were reared at 27 °C and examined daily until all larvae had died or pupated. The ST$_{50}$ was determined by feeding larvae with OBs at a concentration of 3×10^7 OB/ml. Mortality was recorded every 8 h until the remaining survivors pupated. These experiments were repeated in triplicate for each virus.

The LD$_{50}$ values were determined using probit analysis (SPSS Inc., 2003) and compared with a relative median potency method. The ST$_{50}$ was calculated using the Kaplan–Meier estimator and subsequently compared using the log-rank test (SPSS Inc., 2003) [19].

Results

Generation of the *ac114* knockout and positive control AcMNPV bacmids

First, an *ac114*-null bacmid (AcMNPV$^{ac114\text{KO}}$ph$^-$) was generated, and the displacement of *ac114* with the Cm cassette was examined by PCR (Fig. 1b). To test whether the *ac114* knockout would affect OB morphogenesis and to facilitate examination of viral infection, the *polyhedrin* and *gfp* genes were introduced into the *polyhedrin* locus in AcBac-*ac114*KO or AcBac (Fig. 1c). RT-PCR was performed using the primer pairs flanking or within the *ac114* knockout region; the results confirmed that *ac114* had been successfully deleted from the original bacmid (Fig. 1d).

Analysis of AcBac and AcBac-*ac114*KO replication in transfected Sf9 cells

To determine whether the *ac114* knockout had any effect on virus replication, Sf9 cells were transfected with AcBac or AcBac-*ac114*KO. The transfected cells were monitored by the fluorescence output from GFP expression. No difference was observed between the two viruses at 24 h p.t., indicating that the constructs had equal transfection efficiencies (Fig. 2a). For both bacmids, there were gradual increases in the number of infected cells at 72 h p.t., indicating that infectious BVs were produced from the cells that had been initially transfected (Fig. 2a). At 96 h p.t., fluorescence was observed in almost all AcBac or AcBac-*ac114*KO transfected cells (Fig. 2a). Light microscopy analysis at 96 h p.t. showed that OBs with normal appearance had formed in the Sf9 cells transfected with
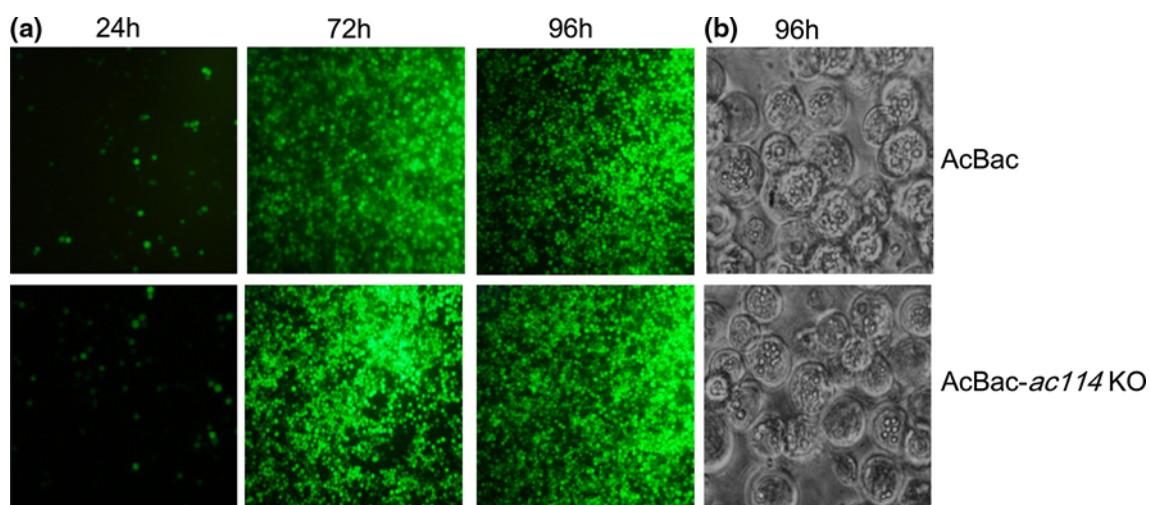

Fig. 2 Analysis of viral replication in Sf9 cells. **a** Fluorescence microscopy of Sf9 cells transfected with AcBac or AcBac-*ac114*KO from 24 h p.t. to 96 h p.t. **b** Light microscopy of OBs in the AcBac or AcBac-*ac114*KO transfected Sf9 cells at 96 h p.t
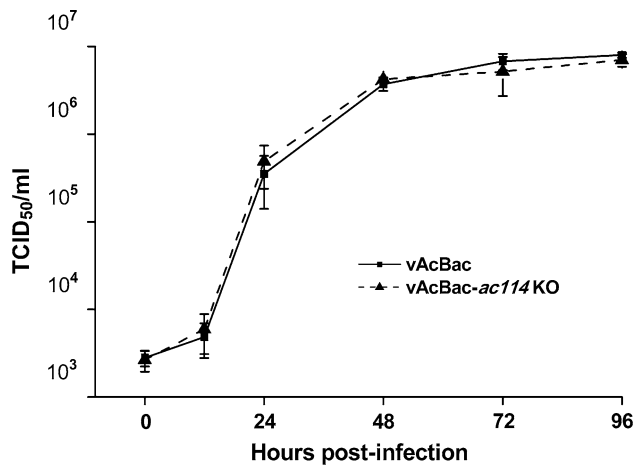
Fig. 3 Viral growth curve analysis. Sf9 cells were infected by vAcBac or vAcBac-*ac114*KO at a MOI of 5. The cell supernatants were harvested at various time points and the titers of the BVs were determined by $TCID_{50}$ end-point assays. Each data point represents the average titer of three independent TCID50 assays. The *bars* represent the standard deviations

both bacmids (Fig. 2b). These results indicate that the *ac114* knockout had no discernible effect on the production of infectious BVs, or the formation of OBs.

To quantify the effect of the *ac114* knockout on virus replication and to determine the replication kinetics of the two viruses, virus growth curves were performed. Sf9 cells infected with the two different viruses showed a steady increase in BV production throughout the infection process (Fig. 3). At each time point, the titer of vAcBac-*ac114*KO was nearly equivalent to vAcBac (all $p > 0.05$). These results indicated that the *ac114* knockout had no apparent effect on BV proliferation in the cultured cells.

Electron microscopy analysis

To examine whether the *ac114* knockout would affect virus morphogenesis, electron microscopy observations were performed on the thin sections generated from the vAcBac-*ac114*KO-infected Sf9 cells. Rod-shaped nucleocapsids associating with the electron-dense edges of the virogenic
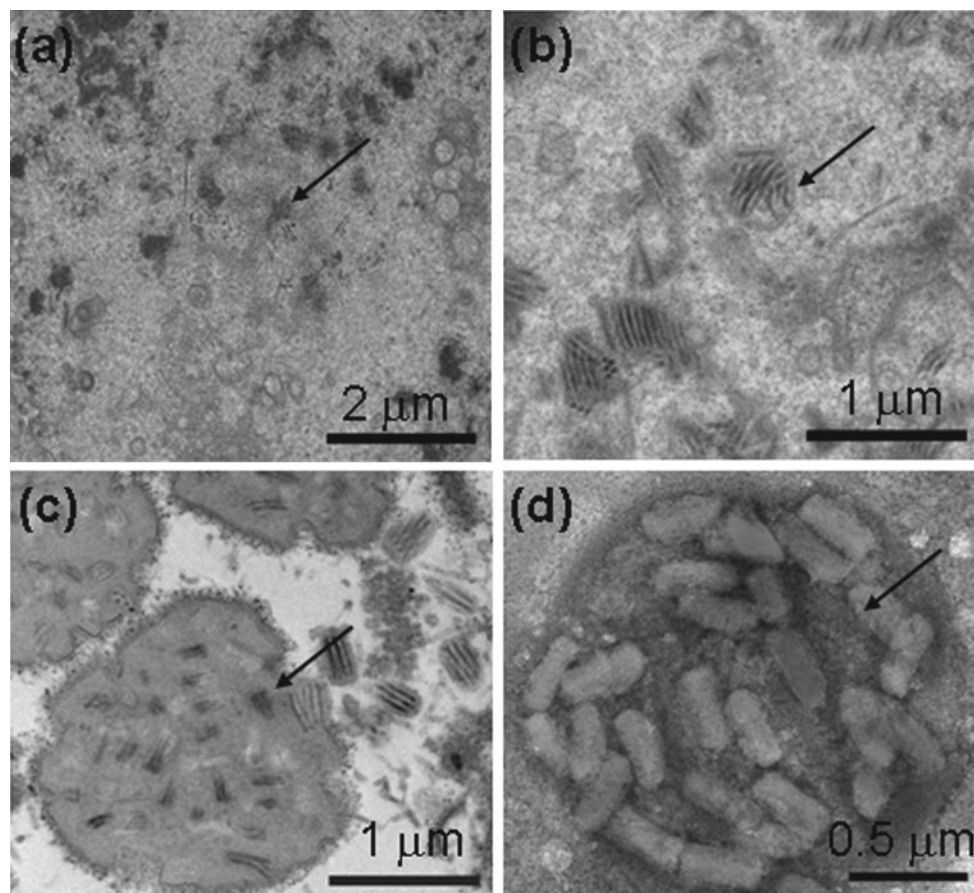

Fig. 4 Electron microscopic analysis of ultrathin sections derived from vAcBac-*ac114*KO-infected Sf9 cells (**a–c**) and alkali-treated OBs extracted from infected *S. exigua* larvae (**d**)
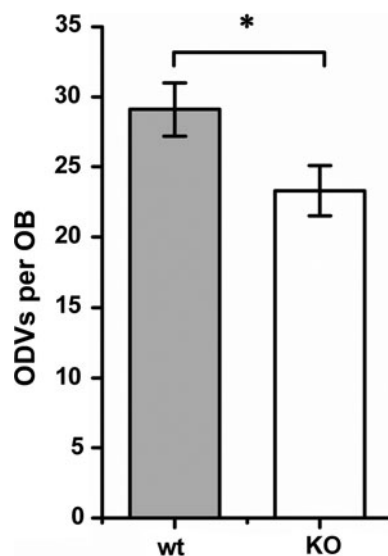
Fig. 5 The comparison of numbers of ODVs per OB between vAcBac and vAcBac-*ac114*KO. Data are shown as means and S.E. ($n = 36$ for each virus; *asterisk* represents that difference is significant, Student's *t* test, $\alpha = 0.05$)

Fig. 6 Transcription analysis of *ac114*. **a** Time course analysis of the transcription profile of *ac114*. Total RNA was extracted from AcMNPV-infected Sf9 cells at designated time points. PCR products from different genes are indicated on the *left*. The sizes of the different PCR products are indicated on the *right*. **b** 5′ RACE analysis of the *ac114* transcript. The transcription initiation site is indicated by an *arrowhead*. The baculovirus late transcription motif is *underlined*

stroma were observed in the nuclei of the vAcBac-*ac114*KO-infected cells (Fig. 4a). The bundles of nucleocapsids were aligning with *de novo* envelopes (Fig. 4b). OBs with normal shapes and sizes were observed; it was also noted that the ODVs had been occluded into the polyhedra within the ring zone (Fig. 4c). ODVs in OBs isolated from vAcBac-*ac114*KO-infected *S. exigua* larvae were observed by dissolving the polyhedron envelope on nickel grids (Fig. 4d). The numbers of virions per OB for vAcBac and vAcBac-*ac114*KO are 29.1 ± 11.5 (mean $\pm$ SD, $n = 36$) and 23.3 ± 10.5 (mean $\pm$ SD, $n = 36$), respectively, which are significantly different ($t = 2.289$, $df = 70$, $p = 0.025$) (Fig. 5).

Transcription analysis

The *orf114* of AcMNPV is 1,275 bp in length and encodes a 424 aa protein with a predicted molecular mass of 48 kDa. Computer analysis showed that a late transcription initiation motif (GTAAG) was found 13 nt upstream of the start codon ATG, suggesting that *ac114* may be a late gene. RT-PCR confirmed that a 1,275 bp *ac114* transcript was detected at 9 h p.i., and was still present at 72 h p.i. (Fig. 6a). 5′ RACE revealed that the transcription initiation site was located 16 nt upstream of the ATG start codon of *ac114* at an A residue (Fig. 6b).

Subcellular localization of Ac114 in Sf9 cells

To investigate the subcellular localization of Ac114, Sf9 cells infected with vAcBac-*ac114*Rep (or vAcBac-*ac114*KO
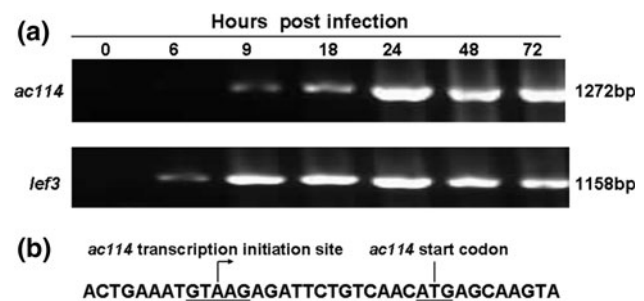
as a control) were observed for GFP expression using fluorescence microscopy. At 96 h p.i., punctate patches of AC114-GFP fluorescence were mostly observed in the cytoplasm of vAcBac-*ac114*Rep-infected cells, whereas GFP fluorescence was evenly distributed in both the cytoplasm and nucleus of the vAcBac-*ac114*KO-infected cells (Fig. 7b).

Effect of the AcMNPV *ac114* knockout on infectivity to *S. exigua* larvae

To determine whether the lack of *ac114* had any effect on the infectivity and killing speed of AcMNPV for third-instar *S. exigua* larvae, bioassays were performed using a droplet-feeding method. In three independent experiments, no significant differences in the ST$_{50}$ values were detected between vAcBac and vAcBac-*ac114*KO (Table 2). However, the LD$_{50}$ of vAcBac-*ac114*KO was significantly higher than vAcBac (Table 3). These results indicate that the loss of *ac114* has an effect on viral infectivity, but does not affect the viral killing speed in *S. exigua* larvae.

Discussion

Homology searches have identified 17 unique genes that are conserved in group I alphabaculovirus, indicating that the function of unique genes may be host dependent [5]. Although *ac114* is one of these unique genes, it is still not known whether *ac114* or its homologs play any roles in the viral infection process. In this study, we demonstrated that *ac114* was not critical for the production of BVs and OBs in vitro. However, interestingly, the *ac114* knockout led to the reduction of viral infectivity in *S. exigua* larvae.

Thus far, few of the unique genes in the group I NPV appear to be directly or indirectly involved in the virus

Fig. 7 Intracellular localization of the *ac114*-GFP fusion protein in Sf9 cells. **a** Schematic diagram of the recombinant bacmid AcBac-*ac114*Rep. The *ac114* orf in frame with the *gfp* gene driven by the *polyhedrin* promoter was inserted into the *polyhedrin* locus of AcMNPV*^{ac114KO}*ph⁻ to generate AcBac-*ac114*Rep. **b** Sf9 cells infected with vAcBac-*ac114*Rep and vAcBac-*ac114*KO were observed under fluorescence microscopy. The nuclear DNA was stained with Hoechst 33258 (*blue*). Cells infected with vAcBac-*ac114*KO were used as a control
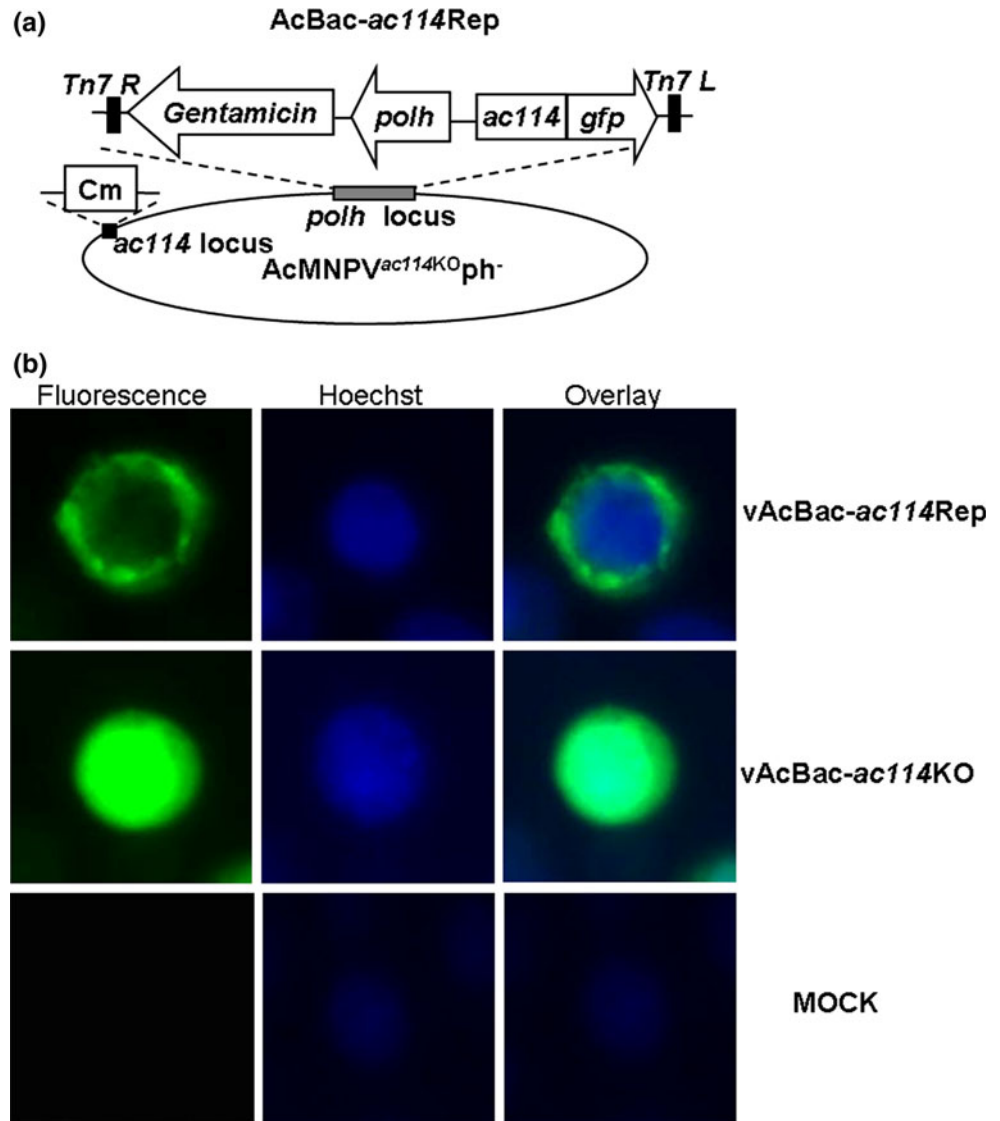
infection process. Mutation of *ie2* in AcMNPV reduced the oral infectivity of OBs in *S. frugiperda* and *Trichoplusia ni* larvae, owing to the absence of virions in the OB [20]. Bm21 of *Bombyx mori* NPV, a homolog of AcMNPV *ac30*, was found not to be essential for virus replication in vitro, but its knockout delayed the killing speed in the larvae [21]. In the present study, we found that the LD_{50} of the *ac114* knockout virus was significantly higher than the control virus. Although Ac114 was identified as a component of BV particle [10], our analysis of the virus growth

Table 2 Time–mortality responses of third-instar *S. exigua* larvae inoculated with vAcBac or vAcBac-*ac114*KO

Bioassay	Virus	ST_{50} (95 %Cl) (h)	χ^2	p
Test 1	vAcBac-*ac114*KO	108 (101–114)	0.31	0.58
	vAcBac	104 (100–107)		
Test 2	vAcBac-*ac114*KO	111 (106–117)	1.21	0.27
	vAcBac	106 (101–110)		
Test 3	vAcBac-*ac114*KO	112 (105–119)	0.03	0.87
	vAcBac	110 (103–117)		

The weights of the larvae used in tests 1, 2, and 3 were 3.16 ± 0.43, 3.27 ± 0.58, and 3.57 ± 0.15 mg, respectively. The digested volumes of the OB suspensions used in tests 1, 2, and 3 were 0.66, 0.82, and 1.07 μl, respectively

Table 3 Dose–mortality responses of third-instar *S. exigua* larvae inoculated with vAcBac or vAcBac-*ac114*KO

Bioassay	Virus	LD$_{50}$ (95 %Cl) (OB/larva)	Relative median potency (95 %Cl)
Test 1	vAcBac-*ac114*KO	290.2 (182.9–499.3)	4.6 (2.3–10.8)*
	vAcBac	63.7 (40.0–99.7)	
Test 2	vAcBac-*ac114*KO	373.4 (226.0–687.2)	5.0 (2.4–12.5)*
	vAcBac	75.2 (46.3–120.1)	
Test 3	vAcBac-*ac114*KO	439.0 (272.4–736.3)	2.8 (1.4–6.5)*
	vAcBac	155.2 (91.6–253.3)	

The weights of the larvae used in tests 1, 2, and 3 were 2.64 ± 0.46, 2.71 ± 0.57, and 3.33 ± 0.43 mg, respectively. The doses of the OB suspension for each bioassay were listed as follows: test 1: 869, 261, 87, 26, and 9 OBs/larva, respectively; test 2: 950, 285, 95, 29, and 10 OBs/larva, respectively; test 3: 850, 255, 85, 26, and 9 OBs/larva, respectively

* 95 % CI of the relative median potency did not include 1.0, indicating that the difference between the LD$_{50}$s was significant

curve detected no significant difference between the *ac114* knockout virus and the control virus, both at MOI = 5 and 2 (Fig. 3 and unshown data), showing that *ac114* knockout did not affect BV production and the increased LD$_{50}$ in the *ac114* knockout virus did not result from the impairment of BV production. Electron microscopic observations found that the numbers of ODVs embedded in one OB between the two viruses were statistically significantly different, indicating that the reduced infectivity of the *ac114* knockout virus, observed in our study based on administration of OBs, might be due to the reduction of virions embedded in the OBs. Ac114 has also been detected as a structural protein of ODV [11], which might interact with one or more of the other ODV proteins and thus affect the efficiency of embedding of ODVs into OBs. It is worth noting that the difference of numbers of ODVs/OB between two viruses was not as dramatic as those of LD$_{50}$ values (Table 3), we cannot exclude the possibility that *ac114* may affect the virus infectivity by other unknown mechanisms. Zhang et al. observed that when AcMNPV orf150 was deleted, from 4- to 18-fold more OBs of mutant virus than wild-type virus were needed to achieve 50 % mortality. They concluded that the difference in virulence was due to the reduction of the number of foci generated by each OB in the primary infection [22].

Transcription analysis of *ac114* by RT-PCR showed that the *ac114*-specific transcript could be detected from 9 to 72 h p.i., indicating that *ac114* was a late transcriptional gene, a result which is consistent with the findings of Jiang et al. [23]. However, a microarray analysis of gene expression in AcMNPV-infected Sf9 cells detected the *ac114* transcript by 2 h p.i., after which time it increased steadily from 12 to 24 h p.i., but then declined [24]. The discrepancy between these studies may result from differences in the AcMNPV genotypes (C6 vs. E2), or in the sensitivity of the detection methods used in the experiments.

The localization assay showed that Ac114 was localized primarily in the cytoplasm of Sf9 cells, a result that is in agreement with the NetNES analysis that detected the leucine-rich nuclear export signal at the C terminus of Ac114 [25]. Our own data verify the localization of Bm94, a homolog of Ac114, which is primarily distributed in the cytoplasm of BmN cells, as displayed by immunofluorescence analysis [26]. It is noteworthy that multiple phosphorylation sites in Ac114 were predicted by Netphos [27]. Phosphorylation modification has been shown to control the nuclear transport of a number of proteins in eukaryotic cells [28]. Whether Ac114 can be phosphorylated and whether its phosphorylation state might regulate its subcellular distribution in Sf9 cells is not known at present.

In summary, this study has shown that *ac114* was not pivotal for the amplification of AcMNPV in vitro, but that it made an effect on the viral infectivity in vivo. To shed light on the potential roles for *ac114* in group I, NPV infection will require further experiments. Such experiments are needed to elucidate whether Ac114 might interact with other proteins and thus participate in the infection process.

References

1. J.A. Jehle, G. Blissard, B. Bonning, J. Cory, E. Herniou, G. Rohrmann, D. Theilmann, S. Thiem, J. Vlak, Arch. Virol. **151**, 1257–1266 (2006)
2. E.A. Herniou, J.A. Jehle, Curr. Drug Targets **8**, 1043–1050 (2007)
3. P.M. de A. Zanotto, B.D. Kessing, J.E. Maruniak, J. Invertebr. Pathol. **62**, 147–164 (1993)
4. M. Ayres, S. Howard, J. Kuzio, M. Lopez-Ferber, R. Possee, Virology **202**, 586–605 (1994)
5. E.A. Herniou, J.A. Olszewski, J.S. Cory, D.R. O'Reilly, Annu. Rev. Entomol. **48**, 211–234 (2003)
6. S.A. Monsma, A.G.P. Oomens, J. Virol. **70**, 4607–4616 (1996)

7. C.Y.-Y. Liu, C.-H. Wang, W.-K. Hsiao, H.-R. Lo, C.P. Wu, Y.C. Chao, J. Virol. **83**, 3604–3616 (2009)

8. S.G. Kamita, K. Nagasaka, J.W. Chua, T. Shimada, K. Mita, M. Kobayashi, S. Maeda, B.D. Hammock, Proc. Nat. Acad. Sci. USA **102**, 2584–2589 (2005)

9. Y. Nie, M. Fang, D.A. Theilmann, Virology **385**, 484–495 (2009)

10. R. Wang, F. Deng, D. Hou, Y. Zhao, L. Guo, H. Wang, Z. Hu, J. Virol. **84**, 7233–7242 (2010)

11. S.C. Braunagel, W.K. Russell, G. Rosas-Acosta, D.H. Russell, M.D. Summers, Proc. Nat. Acad. Sci. USA **100**, 9797–9802 (2003)

12. Y. Jiang, F. Deng, S. Rayner, H. Wang, Z. Hu, Virus Res. **142**, 85–91 (2009)

13. G.F. Rohrmann, *Baculovirus Molecular Biology* (National Library of Medicine (US), National Center for Biotechnology Information, Bethesda, 2008)

14. A.L. Roy, Gene **492**, 32–41 (2012)

15. P.V. Choudary, S.G. Kamita, S. Maeda, *Baculovirus Expression Protocols* (Humana Press, Totowa, 1995)

16. K.A. Datsenko, B.L. Wanner, Proc. Nat. Acad. Sci. USA **97**, 6640–6645 (2000)

17. V.A. Luckow, S.C. Lee, G.F. Barry, P.O.O. Olins, J. Virol. **67**, 4566–4579 (1993)

18. X. Sun, H. Wang, X. Sun, X. Chen, C. Peng, D. Pan, J.A. Jehle, W. van der Werf, J.M. Vlak, Z. Hu, Biol. Control **29**, 124–137 (2004)

19. SPSS Inc., SPSS 12.0 for Windows Users' Guide (SPSS Inc., Chicago, 2003)

20. E.A. Prikhod'ko, A. Lu, J.A. Wilson, L.K. Miller, J. Virol. **73**, 2460 (1999)

21. J. Huang, B. Hao, F. Deng, X. Sun, H. Wang, Z. Hu, J. Gen. Virol. **89**, 922–930 (2008)

22. J.-H. Zhang, T. Ohkawa, J.O. Washburn, L.E. Volkman, J. Gen. Virol. **86**, 1619–1627 (2005)

23. S.S. Jiang, I.-S. Chang, L.-W. Huang, P.-C. Chen, C.-C. Wen, S.-C. Liu, L.-C. Chien, C.-Y. Lin, C.A. Hsiung, J.-L. Juang, J. Virol. **80**, 8989–8999 (2006)

24. M. Iwanaga, K. Takaya, S. Katsuma, M. Ote, S. Tanaka, S.G. Kamita, W. Kang, T. Shimada, M. Kobayashi, Biochem. Biophys. Res. Commun. **323**, 599–614 (2004)

25. T. la Cour, L. Kiemer, A. Mølgaard, R. Gupta, K. Skriver, S. Brunak, Protein Eng. Des. Sel. **17**, 527–536 (2004)

26. G. Liang, G. Li, K. Chen, Q. Yao, H. Chen, Y. Zhou, Curr. Microbiol. **61**, 190–196 (2010)

27. N. Blom, S. Gammeltoft, S. Brunak, J. Mol. Biol. **294**, 1351–1362 (1999)

28. D.A. Jans, S. Hubner, Physiol. Rev. **76**, 651–685 (1996)